Polyelectrolyte Complexes of Ciprofloxacin and Lidocaine Improve Wound Healing in Deep Second Degree Burns and Reduce in Vitro Ciprofloxacin Cytotoxicity in Fibroblasts

María Florencia Sanchez
Unidad de Investigación y Desarrollo en Tecnología Farmacéutica (UNITEFA), CONICET and Departamento de Ciencias Farmacéuticas, Facultad de Ciencias Químicas, Universidad Nacional de Córdoba

María Laura Guzman
Unidad de Investigación y Desarrollo en Tecnología Farmacéutica (UNITEFA), CONICET and Departamento de Ciencias Farmacéuticas, Facultad de Ciencias Químicas, Universidad Nacional de Córdoba

Jesica Flores-Martín
Universidad Nacional de Córdoba, Facultad de Ciencias Químicas, Departamento de Bioquímica Clínica and Centro de Investigaciones en Bioquímica Clínica e Inmunología (CIBICI), CONICET

Mariano Cruz Del Puerto
Universidad Nacional de Córdoba, Facultad de Ciencias Químicas, Departamento de Bioquímica Clínica and Centro de Investigaciones en Bioquímica Clínica e Inmunología (CIBICI), CONICET

Carlos Laino
Instituto Nacional de Biotecnología, Centro de Investigación e Innovación Tecnológica (CENIIT), Universidad de La Rioja

Elio Andres Soria
Instituto de Investigaciones en Ciencias de la Salud (INICSA), CONICET and Facultad de Ciencias Médicas, Universidad Nacional de Córdoba

Susana Genti-Raimondi
Universidad Nacional de Córdoba, Facultad de Ciencias Químicas, Departamento de Bioquímica Clínica and Centro de Investigaciones en Bioquímica Clínica e Inmunología (CIBICI), CONICET

María Eugenia Olivera (✉ eugenia.olivera@unc.edu.ar)
Unidad de Investigación y Desarrollo en Tecnología Farmacéutica (UNITEFA), CONICET and Departamento de Ciencias Farmacéuticas, Facultad de Ciencias Químicas, Universidad Nacional de Córdoba

---

Research Article

Keywords: Drug delivery systems, dressings, alginates, hyaluronate, wound healing, burns

Posted Date: January 7th, 2022

DOI: https://doi.org/10.21203/rs.3.rs-1197328/v1

Abstract

The development of new treatments capable of controlling infections and pain related to burns continues to be a challenge. Antimicrobials are necessary tools, but these can be cytotoxic for regenerating cells.

In this study, antibiotic-anesthetic smart systems obtained by ionic complexation of polyelectrolytes with ciprofloxacin and lidocaine were obtained as film and hydrogel. The complexation of ciprofloxacin with natural polyelectrolytes efficiently contributed to increasing biocompatibility in a primary culture of isolated fibroblasts. In addition, the relative levels of the proteins integrin β1 and p-FAK involved in cell migration were increased with no modifications in cell mobility. Their evaluation in a deep second-degree burn model revealed fast reepithelization, with appendage conservation and complete dermis organization. Encouragingly, we found that both the film and the hydrogel showed a significantly superior performance compared to the reference treatment of silver sulfadiazine cream.

This work highlights the great potential of this smart system as an attractive dressing for burns, which surpasses currently available treatments.

1. Introduction

Wounds are susceptible to infections, and their treatment is important because infections can slow down the rate of wound healing. Concerning burns, most non-complicated superficial second degree ones will heal spontaneously or after a conservative treatment[1]. In deep partial thickness burns, there is damage to the deeper structures of the dermis, involving sweat glands and hair follicles, and these take more than 2-3 weeks to heal. Thus, they are more likely to result in scarring with functional and psychological consequences[2]. Therefore, a topical therapy that supports sustained antimicrobial activity would prevent infections and facilitate wound healing[3]. The antimicrobial choice should be taken with caution, since, in addition to its bactericidal activity, antimicrobials can produce eukaryotic skin cell death, thereby preventing tissue regeneration. The level of toxicity depends on its specificity and its mechanism of action[4].

The gold standard for topical treatment of second degree burns is silver sulfadiazine. However, its use has been systematically questioned, mainly due to the lack of selectivity of its cytotoxic mechanisms[5,6]. In this sense, new elemental silver-based dressings are more biocompatible, but still deficient in promoting wound healing as a result of the high cytotoxicity of silver to skin cells[4,5].

Biomaterials, such as polyelectrolytes, can be utilized as carriers to obtain systems with a modified release of antimicrobials. This specific and regulated release strategy can reduce the cytotoxicity of the antimicrobials[7]. In this sense, ciprofloxacin-based PE dressings were proposed for wound healing and have shown good biocompatibility and antimicrobial properties[8,9]. In previous studies, an antibiotic-anaesthetic hydrogel (AA-hydrogel) and antibiotic-anaesthetic film (AA-films) were developed. In both cases, the ionic interactions established between the PE and drugs allowed sustained-release antibiotic-

anesthetic systems to be obtained with potential applications in wound healing. AA-hydrogel revealed faster reepithelization of superficial second degree burns than those treated with silver sulfadiazine, as well as providing pain relief[10]. AAfilms as wound dressings have the advantages of easy and non-invasive application and dose accuracy. In addition, AA-films are transparent, compatible with wound skin pH, highly water vapor permeable, have a high fluid absorption capacity that acts as a physical barrier for microorganisms, and the *in vitro* antimicrobial efficacy against *S. aureus* and *P. aeruginosa* has been demonstrated[11]. However, neither of these two systems has been evaluated in deep second degree burns. Moreover, it is not known what impact PE with drug complexation might have on eukaryotic cells.

The objective of this work was to evaluate the wound healing performance of these AAfilms. To this end, we used a deep second degree burn experimental model, which was compared with the reference treatment and a primary culture of isolated fibroblasts in order to study cell viability and migration. We found that AA-hydrogels and films facilitated wound repair with safety and efficacy, which means that they could be considered as potential treatments in clinic.

2. Results And Discussion

2.1. Cytotoxicity of Cip, PE and PE-Cip in HDF cells

2.1.1. Polyelectrolyte cell compatibility

Initially, we evaluated HDF cell viability when these cells were exposed to treatments with low (0.01% p/p, PE_L) or high (0.1% p/p, PE_H) concentrations of CB, SA, and SH.

The PE_L concentrations did not modify the cell viability related to the control (Figure 1). In the case of SH_H, the HDF cell viability was even slightly increased (15%), suggesting excellent biocompatibility properties. In agreement, Guo et al (2015)[12] observed the same tendency in the mouse fibroblast line L929. The increase in HDF cell viability in the presence of SH may be related to its endogenous nature, since it is the most relevant structural element of the extracellular matrix[13]. In fact, HDFs have SH primary cell receptors (CD44 and RHAMM) that are involved in the modulation of complex biological functions such as cell migration and proliferation, inflammation and tumorigenicity[14].

Good cell compatibility was also evident in the presence of SA_H, which produced no changes in HDF cell viability. These results are not in agreement with Guo et al (2015)[12], where SA 0.1% (SA_H) reduced viability to approximately 70%. Such differences could be due to the cell line used (mouse fibroblast L929), to differences in viscosity or in monomeric composition (manuronic:guluronic ratio), or to combination of these. In contrast, cell viability decreased to 65% with CB_H, which implied a low in vitro biocompatibility. Similar results were observed by Guo et al (2015)[12] in a mouse fibroblast line L929, which could be assigned to the characteristic higher viscosity of synthetic polyelectrolytes, which generates three-dimensional structures covering living cells and hindering the arrival of culture medium

nutrients, thereby reducing the metabolic activity or blocking the transport of vital molecules to cells[15]. However, it is important to note that this in vitro phenomenon may not necessarily occur in an in vivo condition, where the nutrition of the cells in a tissue comes from the extracellular matrix components. In fact, the healing of second-degree superficial burns treated with an hydrogel of carbomer combined with Cip and lidocaine (CbNaCipLid) has shown a fast and complete regeneration[10].

2.1.2. Cell compatibility of Cip and PE-Cip complexes

The addition of Cip_3 to cell cultures produced a non-cytotoxic effect (Figure 2A), whereas Cip_{30} treatment significantly reduced cell viability by up to 60% (Figure 2B). In this regard, it has been reported that Cip inhibits cellular functions, thus preventing the growth of mammalian cell lines. Cip also induces mitochondrial dysfunction and oxidative damage in a dose-dependent manner. However, this toxic effect can be counteracted by the exogenous incorporation of vitamin E as an antioxidant[16,17].

Next, we evaluated the HDF cell viability of Cip at 3 µg/mL or 30 µg/mL in the presence of PE. No cytotoxic effect was observed when Cip 3 µg/mL was combined with PE, except for CB_H-CIP_3, which followed the same pattern as CB_H alone. A slight cell viability reduction was observed for SA_L-CIP_3 and SA_H-CIP_3. However, these were not cytotoxic since the values were higher than 70% (Figure 2A).

Interestingly, at higher cytotoxic concentrations of Cip_{30}, a significant increase in HDF cell viability was revealed in the presence of PE_L and PE_H, with the only exception being CB_H-Cip_{30}, whose non-significant increase in viability was still below 70% (Figure 2B).

The increase in HDF cell viability by PE-Cip complexes with respect to Cip alone suggests that these PE have a protective effect, which could be due to the ability of SA and SH to counteract the cellular damage produced by the reactive oxygen species arising from the presence of Cip[18,19]. In addition, the PE-Cip interaction can reduce free Cip concentrations in the medium[20], so a combination of both mechanisms cannot be ruled out.

2.2. Effect of PE and its PE-Cip complexes on HDF cell migration

To analyze the effect of PE alone and its Cip complexes on HDF cell migration, wound healing assays were performed. As shown in Figure 3A, the cell treatment with SA or SH at high doses or in the presence of Cip_{80} did not alter the cell ability to heal the wound compared with the control; whereas, the addition of CB, $Cip_{80,}$ or CB-Cip_{80} to the cell culture significantly decreased the cell migration compared to the control. The quantitative analyses of pooled data of three independent experiments are shown in Figure 3B. Consistent with the Cip effect on HDF cells, Chen et al (2016)[21] reported that Cip also notably reduced the migration of human corneal fibroblasts. The decrease in the cell migration observed for CB alone or with CIP_{80} may have been due to a Cip cytotoxic effect on the cells (see Figures 1 and 2), although an impact

of the high viscosity of CB cannot be discarded. Related to this, it has been reported that cell mobility is directly reduced when cells are grown in a medium with high viscosity[22].

2.3. Effect of PE and its PE-Cip complexes on the protein expression implicated in cell migration

Integrin β1 and p-FAK is a signaling pathway involved in new focal adhesions formation and cell migration[23]. To establish the effect of the different treatments on the expression of the main proteins involved in cell migration, western blot assays were performed. Figure 4A shows representative images of integrin β1 and p-FAK expression in HDF cell cultures. The results indicate that cells exposed to Cip_{80}, the CB_H dose or its CB_H-Cip_{80} complex presented similar integrin β1 levels to the control cells; whereas cells treaded with SA_H and SH_H of their respective PE-Cip_{80} complexes had significantly increased integrin β1 levels compared to the control (Figure 4B). Regarding p-FAK expression, all the treatments revealed increased levels, related to the Cip_{80} exposed cells (Figure 4C).

These data are consistent with those observed with the in vitro wound healing assays. In addition, they suggest that these in vivo treatments may be accelerating wound closure. One of the first proteins that was identified downstream of integrin stimulation is FAK. This is a nonreceptor tyrosine kinase that localizes to the sites of integrin-mediated adhesion to the ECM. Activation of FAK results in increased cell motility and survival, as well as other cell responses involved in wound healing[24]. Taken together, these findings suggest that PE-Cip complexes are triggering a signal transduction cascade that promotes focal adhesions and regulates cell mobility. Although the in vitro systems cannot be directly extrapolated to the in vivo conditions, since it is not possible to reproduce exhaustively the tissue physiology, the in vitro test conditions provide greater sensitivity to antimicrobial toxicity than would be expected to found in in vivo systems.

2.4. Wound-healing *in vivo* test

2.4.1. Macroscopic wound healing study

Although most non-complex burn injuries will heal spontaneously or after a conservative treatment[1], several studies have shown that wounds that take more than 2-3 weeks to heal are more likely to result in scarring with functional and psychological consequences[2]. The management of burn wounds has a considerable influence on the time taken for the wound to heal[6], so a good initial care will have a positive influence on the outcome[25].

No signs of pain or general discomfort were observed in any animal during the trial, with the behavior (in terms of food and water intake and daily activity) being normal. In addition, no clinical signs of infections were observed. Figure 5 shows the wound healing results for each treatment after 7, 14, and 21 days-post burn.

On day 7, the wound area had slightly increased in the NT group, possibly due to local inflammation. However, with the exception of R-cream, the treatments with AAfilms, Cfilms, and AAhydrogel significantly reduced the wound areas faster than NT ($p < 0.05$). On day 14, no significant differences were observed with respect to NT, with R-cream being less effective in closing wounds than the other treatments ($p < 0.05$). Moreover, the R-cream group revealed a more open wound area at the trial end, even with respect to the NT group, on day 21 ($p < 0.05$).

All open wounds are an ideal environment for microbial colonization[3,26]. Thus, the early closure observed from day 7 supports a beneficial effect of the polyelectrolytes. Also, these treatments proved to be better than the standard one (Rcream), which was not effective in closing wounds at 21 days post burn. A faster closure involves cellular proliferation and migration, which is critical for restoring the barrier function and for minimizing the risk of burn wound infections[4,6].

2.4.2. Microscopic wound healing study

To characterize further the healing process, the wounds were also analyzed microscopically. The epidermal evolution is shown in Figure 6, with the treatments being significantly associated with the epidermal scores ($p < 0.005$).

On day 7, the NT group showed an absent or discontinuous epidermis at similar frequencies, whereas all animals treated with AAfilms and AA-hydrogel already presented a discontinuous epidermis. Although the C-film group included some animals having an absent epidermis, most of these animals showed epidermal recovery to different extents. In contrast, the Rcream group revealed an absent epidermis in all cases.

On day 14, in the NT group, animals with a previous discontinuity evolved to a continuous epidermis, while those with a previously absent one evolved to a discontinuous epidermis. The AAfilms and AA-hydrogel treatment led to permanent recovery, whereas the C-film treatment achieved this to a lesser extent (on days 14 and 21). On the other hand, R-cream showed an inconstant and only partial epidermal recovery in the last 2 weeks.

On day 21, the NT group achieved complete healing, as the AAfilms and AAhydrogel had done earlier, with their effects being maintained up to the trial end. Thus, the treatments exerted an earlier and sustained epithelialization in all cases, with the polyelectrolytes accompanied by active principles being the most effective. These results are in agreement with the above-mentioned macroscopic outcomes.

In association with epithelialization, dermal regeneration is mainly carried out by the migration and proliferation of fibroblasts. In addition, collagen and some other components of the extracellular matrix are also required to close the wound efficiently. Nonetheless, a fibrotic over-response can deleteriously lead to dense skin scars. The dermis also contributes to appendage regeneration and the biomechanical properties of the regenerated skin, which affect its quality[27]. If the new tissue is very different to the

normal skin, the functionality will be compromised[25], with poor aesthetic results and psychological sequels for the patient[2].

Figure 7 shows the dermal regeneration scores, with treatments being significantly associated with the scores ($p< 0.05$). On day 7, there were no differences among AAfilms, C-films, and AA-hydrogel, which revealed more animals with reticular recovery than the NT group or R-cream, with half of these groups still showing complete dermal disorganization.

On day 14, the AAfilms presented advanced dermal healing with scores of 4 or 5; whereas R-cream, C-films, and AA-hydrogel exerted skin recovery (scores of 3 or 4). On the other hand, the NT group showed a heterogeneous effect, with scores ranging from 1 to 4.

On day 21, the disorganized skin of the NT group evolved to recovery in the reticular and papillary layers. The R-cream group presented skin score involution, which was in agreement with the epidermal scores and macroscopic healing. In contrast, the AAfilms and AAhydrogel led to an increase in the frequency of animals with normal skin (a normal reticular dermis was found in all cases), promoting dermal remodeling with respect to groups with no treatment or the standard one.

Figure 8 shows representative photomicrographs of each experimental group, which support the results shown in Figures 7 and 8. The NT group exhibited a low definition between the reticular and papillary dermis, as well as with appendage hemorrhage occurring on day 7 post burns, which then presented cellular infiltration that evolved to a dense scar without skin appendages over the following days. Although the epidermis was continuous at the trial end, it had an atypical structure.

Concerning the R-cream group, despite this being considered the gold standard treatment for burns, it was significantly less effective than the other treatments. Moreover, wound healing was delayed compared with the NT group, with the skin recovery observed on day 14 being transient and with a later impairment on day 21 being accompanied by cellular infiltration. This is in fact a frequent problem related to the repeated application of silver sulfadiazine creams and silver-based dressings, which are deleterious to keratinocytes and fibroblasts[5,28], partly due to the hydrophobic nature of the vehicle and the unspecific killing action of silver[9,29,30].

The main outcome found in animals treated with AAfilms (with respect to the previous treatments) was an early epidermal and dermal healing on day 14 with appendage conservation, which then allowed the normal reticular and papillary dermis to be differentiable. Also, the epidermis was well-differentiated with clear basophilic staining and a corneal layer. The AA-hydrogel and C-films achieved similar outcomes, but to a lesser extent.

Wound healing in C-film-treated burns was superior to that found in the R-cream group, despite not having an antimicrobial in the composition. This demonstrated the beneficial healing effect of sodium alginate or sodium hyaluronate polysaccharides, which is due to several mechanisms, and is consistent with numerous scientific reports[7,29,31]. In this regard, the moist wound environment generated by films, as well

demonstrated by the in vitro assays, was convenient for cell viability and physiology[2,32]. Furthermore, systems based on polymers are well-known for their ability to cool the skin surface by absorbing and dissipating the heat. This reduces the inflammatory response and limits tissue damage, resulting in faster regeneration[33] and an improved well-being for the patient[33–35]. These benefits were increased by AAfilms, which indicated that neither ciprofloxacin nor lidocaine interfered with skin healing and could actually improve this by ciprofloxacin antimicrobial activity. This shortened evolution might prevent further development of chronic wounds and the risk of bacterial dissemination, thereby improving patient prognosis. Nevertheless, it still remains to be seen whether this system can promote faster wound healing and exhibit antimicrobial effects on an infected wound in vivo. It should be taken into account that these results were obtained in a rat burn model, whose most significant limitation is the subcutaneous panniculus carnosus muscle that facilitates skin healing by both wound contraction and collagen formation. However, this rapid wound contraction allows to study the mechanics of wound healing and to compare the performance of alternative treatments[36].

The present investigation took advantage of the ionic interaction established between a polyelectrolyte and certain drugs to develop new materials with potential applications in clinic. Although both the AAfilms and AA-hydrogel promoted skin healing, the films show more advantages as wound dressings, such as their easy and noninvasive application and dose accuracy. The development or optimization of advanced dressings still represents a very active research field, with the aim being to improve skin healing in relation to specific clinical applications. Related to this, numerous new systems containing peptides, growth factors or cells[25,37,38] have been proposed in the scientific literature as improved alternatives for the treatment of wounds in general, and have demonstrated the ability to increase wound healing. Compared with these antecedents, the AA-film development has revealed several advantages, such as being an economic, simple and robust manufacturing process accomplished by the rational selection of materials and the knowledge of their chemical and biological characteristics. It can thus be suggested that the design films made from biomaterials with antimicrobials and anesthetics with extended-release and a sound manufacturing process is a promising development for the improvement of burn pharmacotherapy. Moreover, from a technological and pharmaceutical point of view, the use of these biomaterials and drugs approved by regulatory health authorities constitutes a translational medicine approach with a great potential for advancing to the productive sector, with the possibility of becoming a new alternative use of the drugs.

3. Materials And Methods

3.1. Materials

Ciprofloxacin hydrochloride was donated by Bago® laboratory (Argentina). Cip as a base was obtained from ciprofloxacin hydrochloride according to Sanchez et al [10]. Lidocaine hydrochloride, Carbomer 974P NF (CB), $CaCl_2$ and sodium hyaluronate (SH) were obtained from Parafarm® (SH, Argentina). Sodium alginate (SA) was purchased from Sigma Aldrich® (SA, USA). Anhydrous glycerol 99.5% was obtained

from Cicarelli® (Argentina). The 0.9% NaCl sterile solution was from Braun® (Argentina), and ethanol 70 v/v was diluted from 96 v/v (Bialcohol, Porta®, Argentina) according the Argentinian Pharmacopeia, 7º edition (FA7)[39]. All these chemical reagents and solvents used were of pharmaceutical or analytical grade. Ultrapure water was obtained from a water purification system (Heal Force®, China) and sterilized.

3.2. Preparation of PE-Cip systems for cell culture

The PE-Cip systems were obtained as follows: water dispersions of PE (CB, SA or SH) were prepared at different concentrations. Then, an aqueous suspension of Cip was added under stirring until the disappearance of the Cip particles. Also, dispersions of PE alone or of CipHCl solutions (in equivalent Cip concentrations) were obtained. Finally, 1:10 dilutions were made with culture medium (Table 1).

Table 1
PE-Cip treatments

Assay	Cip concentration	PE*	PE_L-Cip systems	PE_H-Cip systems
Cell viability	3 µg/mL (Cip_3)	0.01% (PE_L)	PE_LCip_3	PE_HCip_3
	30 g/mL (Cip_{30})	0.1 % (PE_H)	PE_LCip_{30}	PE_HCip_{30}
Wound healing scratch	80 µg/mL (Cip_{80})**	0.1% (PE_H)	–	PE_HCip_{80}

*PE are CB, SA, or SH; PE_L (means PE low concentration) and PE_H (means PE high concentration), ** Due to the greater number of cells per plate required for the wound healing scratch assay, the highest concentration of Cip that was able to dissolve in the culture medium was used [40].

3.3. Cell culture

Normal Human Dermal Fibroblasts (HDF) were kindly provided by Dr. Donadio from the Departamento de Bioquímica Clínica, Facultad de Ciencias Químicas, Universidad Nacional de Córdoba (FCQ-UNC) and Centro de Investigación en Bioquímica Clínica e Inmunología (CIBICI-CONICET). HDF were obtained from anonymized healthy volunteers who gave informed consent with the protocol being approved by the Ethical Committee of Hospital Nacional de Clínicas, Universidad Nacional de Córdoba[41]. All experiments were performed in accordance with the guidelines and regulations of the Council for Ethical Evaluation of Health Research (CoEIS, Health Ministry of the Province of Córdoba) and in compliance with Provincial Law 9694. The cultivated cells were used between passages 4 and 6. HDF cells were cultivated in Dulbecco's Modified Eagle's Medium (DMEM, Gibco®) supplemented with 20% (v/v) fetal bovine serum (FBS, Natocor®), 100 µg/ml penicillin and 100 µg/ml streptomycin (Invitrogen) at 37°C and 5% CO_2 (SANYO® MCO-17AC, Germany).

3.4. Study of cell compatibility: cell viability assay

To evaluate cell viability, 1 x 10^6 cells were cultured in 96-well plates (~80% of confluence) for 24 h. Then, the cells were treated with different PE-Cip conditions (Table 1) for 24 h, and cell viability was evaluated using the metabolic dye 3-(4,5-dimethylthiazol-2-yl)-2,5-diphenyl tetrazolium bromide (MTT) assay. Briefly,

an MTT solution (1 mg/mL MTT in phosphate buffered saline, Sigma-Aldrich) was added to each well (1:10) and incubated for 2.5 h at 37 ºC. After this incubation, the media were removed and the formazan precipitated was dissolved in 100 µL of dimethylsulfoxide (DMSO, Cicarelli). Absorbance was measured at 540 nm, and the results were expressed as the percentage of cell viability (CV%) relative to the control, according Equation 1. Two independent experiments were conducted in quadruplicate (n=8).

$$CV\% = \frac{\left[A_{sample}\right]}{\left[A_{control}\right]} \times 100\% \quad \text{Equation 1}$$

where $[A_{sample}]$ and $[A_{control}]$ represent the absorbance measured in treated and untreated cells, respectively.

According to ISO 10993-5[42], the lower the CV% value, the higher the cytotoxic potential of the test item is. If viability is reduced to <70% of the blank, it has a cytotoxic potential.

The statistical analysis was carried out using GraphPad Prism® v.7.00 software. For the cell viability assay, data were expressed as the mean ± SEM (n=8). The differences among the treatments were analyzed by ANOVA and Tukey's post hoc test.

3.5. Effect of PE and its PE-Cip complexes on HDF cell migration.

3.5.1. Wound healing scratch assay in cell culture

The migratory potential of fibroblasts was assessed by a wound healing scratch assay as described by Flores-Martín et al[43]. Briefly, 3 x 10^5 cells were cultured in 24-well plates for 24 h, after which, two parallel scratches were made in the confluent monolayer of each well with a plastic disposable pipette tip (10 µL). The cultures were washed twice with phosphate buffered saline (PBS, Sigma®) to remove all detached cells, and cultivated under different PE-Cip conditions (the culture medium had only 2% of SFB in order to minimize cell growth) for 24 h (Table 1).

The wound area was photographed at t=0 h and t=24 h, with a microscope coupled to a LEICA® (DMI 8) digital camera. The pictures were analyzed using ImageJ v.1.51c software (National Institute of Health), and the migrated area % (MA%) was calculated according Equation 2. Three independent experiments were conducted in quadruplicate (n=12).

$$MA\% = \frac{\left[Area_{24h}\right]}{\left[Area_{0h}\right]} \times 100\% \quad \text{Equation 2}$$

where $[Area_{0\,h}]$ is the area at t=0 and $[Area_{24\,h}]$ is the cell-populated area after 24 hours of the test. MA% vs treatments were plotted with GraphPad Prism® v.7.00 software.

Effect of PE and its PE-Cip complexes on the protein expression implicated in cell migration. SDS-PAGE and Western Blot.

Whole protein extracts were prepared in sample buffer (2x Laemmli buffer containing 2-β-mercaptoethanol) as described in Flores-Martín et al (2012)[43], and protein samples were loaded onto a 10% SDS-PAGE gel. After migration, the proteins were electrotransferred to nitrocellulose (Amersham Bioscience). The membrane was blocked for 1 h with 5% v/v non-fat dry milk in Tris buffered saline (TBST) (25 mM Tris, 150 mM NaCl, 2 mM KCl, pH 7.4, containing 0.2% v/v Tween-20), washed, and incubated with each of the following primary antibodies: mouse monoclonal anti-integrin β1 (dilution 1/300 v/v; sc-374429 Santa Cruz Biotechnology®); rabbit polyclonal anti-pFak Tyr 397 (dilution 1/200 v/v; sc-11765-R, Santa Cruz Biotechnology®); and mouse monoclonal anti-α-tubulin (dilution 1/5000 v/v; clon B512, Sigma-Aldrich®). After washing with TBST, blots were incubated with IRDye 800CW donkey anti-rabbit IgG (1:10000; P/N 926-32213, LI-COR Biosciences) or IRDye 680RD donkey anti-mouse IgG (1:10000; P/N 926-68072, LI-COR Biosciences) antibodies in TBS for 1 hour, protected from light. After two washes with TBST and one with TBS, the membranes were visualized and quantified using the Odyssey Infrared Imaging System (LI-COR, Inc., Lincoln, NE, USA). Protein expression was normalized to the α-tubulin levels. The relative levels of proteins vs treatments were plotted with GraphPad Prism® v.7.00 software.

3.5.3 Statistical analysis

In the wound healing scratch assay, the data were expressed as the mean ± SEM (n=12). The differences among the treatments were analyzed by Kruskal-Wallis and Dunn's post hoc test. In SDS-PAGE and *Western Blot*, the data were expressed as the mean ± SEM (n=6). The differences among these treatments were analyzed using ANOVA and Dunnett's post hoc test. In all cases, $p<0.05$ was considered statistically significant.

3.6. Preparation of the AAfilms and AA-hydrogel for the *in vivo* assay

The AA-films were prepared by the casting technique according to Sanchez et al (2021)[11]. For comparison, the same hydrogel, but without the drugs, was also prepared and used as a control (C-films)[11]. The AA-hydrogel was prepared according to Sanchez et al (2018)[10]. A cream with 1.00% silver sulfadiazine, 0.66% lidocaine and 248000 UI vitamin A (Platsul A® cream, Souberian Chobet S.R.L., Batch nº 11318, Argentina) was used as a reference treatment (R-cream).

3.7. Wound-healing *in vivo* test

An experimental murine model of deep second degree burns was used[44]. The studies were conducted according to ethical protocols described in the National Institutes Health guide for the care and use of

experimental animals[45] and in compliance with the ARRIVE guidelines. In addition, the trial was approved by the Ethics Committee CICUAL of the University of La Rioja (Protocol nº 5/18).

Healthy male Wistar rats, with a weight of between 250 and 300 g, were placed into cages with a physical division to avoid contact between animals, kept in a room with controlled temperature (21 ± 5°C), and exposed to light/dark cycles of 12 h. To minimize the risk of infection, the wood sawdust of the cages was changed three times per week. Animals had free access to food and water.

On day 0, the rats were anesthetized with an intraperitoneal injection of 85.0 mg/kg ketamine (Ketamina 50® Holliday-Scott, 50 mg/mL) plus 6.0 mg/kg xylazine (Xilacina 20® Richmond, 20 mg/mL), according to Yaman et al (2010)[44]. Then, the lower dorsal region of each animal was shaved and then cleaned with 70 v/v ethanol. A deep second degree burn was made by exposure to a metal device for 30 seconds without additional pressure (cylinder 1 cm in diameter, 10 g, pre-heated by immersion in boiling water). The metal device temperature (90 ± 2) ºC was measured with the infrared thermometer ST882 (Reed Instruments®, USA). Finally, the burns were cleaned with sterile gauze soaked in 0.9% NaCl sterile solution. Immediately after, the animals were randomly divided into the 5 groups as described below in Table 2.

Animals of the AA-film and C-film groups were treated with a circular portion of these films cut with a 12 mm ø punch. The AA-hydrogel and R-cream groups were treated with 0.2 mL of the corresponding treatment applied with a 1-mL syringe. Before each treatment application, the wounds were cleaned with sterile gauze soaked in 0.9% NaCl solution. The treatments were repeated once a day for 21 days. Investigators could not be blinded because the topical treatments were easily distinguishable from each other; i.e. R-cream is a white semisolid, AA-hydrogel is a transparent semisolid, and AA-films and C-films are solid transparent circular portions of films. At the end of the experiment, the animals were sacrificed with a lethal dose of the anesthetics.

Table 2
Assignment of experimental treatments.

Group	Nº animals
AAfilms	6
C-films (control, drug-free films)	6
AA-hydrogel	3
R-cream (reference treatment)	6
NT group (no treatment, negative control)	6

3.7.1. Macroscopic wound healing in vivo study

Animal behavior was observed each day. Also, the appearance, color, hair growth and clinical signs of a possible infection process (heat, redness, and swelling) of the wounds were recorded. On days 0, 7, 14, and 21, the wounds were photographed with a Nikon d3200 camera (Japan), with a ruler being placed for enable further analysis. The wound area was measured from these photographs using Image J v1.51j8 software (NIH, USA), and the wound healing was calculated according to Equation 3:

$$Macroscopic\ wound\ healing\ (\%) = \frac{[Area_t]}{[Area_0]} \times 100\% \quad \text{Equation 3}$$

where $[Area_0]$ is the wound area on day 0 and $[Area_t]$ is the wound area on days 7, 14 or 21. The mean macroscopic wound healing ± SD (n=6) versus time was plotted. Treatments were compared at each time recorded using ANOVA followed by Fisher's test with a significance level of $p< 0.05$, utilizing InfoStat® v.2012 software (InfoStat Group, Argentina).

3.7.2. Microscopic wound healing in vivo study

Burned skin tissue biopsies (3 mm) were collected under anesthesia on days 0, 7, 14, or 21, as shown in Figure 9. These samples were fixed in 10% neutral buffered formalin, dehydrated by serial immersion, embedded in paraffin, and cut with a microtome into 5 µm sections. These sections were subsequently processed using the hematoxylin-eosin universal technique. Then, photomicrographs were taken at

100x magnification using the BX41 optical light microscope (Olympus®, Japan).

The epidermal continuity and dermal regeneration were obtained from 6 fields of each biopsy and were scored as the relative frequency of cases according to Table 3.

The Chi-square method was used to establish statistical associations between the histological scores and treatments. The Cochran-Mantel-Haenszel test was used in the time-stratified analysis of the epidermal and dermal scores to evaluate the association between treatments and score frequencies for $p< 0.05$. Statistical probes were performed using the InfoStat® v.2012 software (InfoStat Group, Argentina).

Table 3
Epidermal and dermal histological assessment scores.

Tissue	Score	Description
Epidermal continuity	1	Absent
	2	Discontinuous
	3	Continuous
Dermal recuperation	1	Complete dermal disorganization
	2	Reticular recovery, papillary disorganization
	3	Recovery of reticular and papillary dermis
	4	Normal reticular dermis with papillary recovery
	5	Completely normal dermis

Declarations

Declaration of Competing Interest

The authors declare that they have no known competing financial interests or personal relationships that could have appeared to influence the work reported in this paper.

Acknowledgements

To Dr. Ana Carolina Donadio, for the kind provision of the HDF cells. The authors also thank Dr. Luciana Reyna, Dr. Paula Abadie, Dr. Gabriela Furlán, and Dr. Laura Gatica for technical assistance, and Dr. Cecilia Sampedro, Dr. Carlos Mas and Dr. Pilar Crespo from the Centro de Micro y Nanoscopía de Córdoba-CEMINCO- CONICET-Universidad Nacional de Córdoba, Córdoba, Argentina for technical and imaging assistance.

This study was supported by grants from the Agencia Nacional de Promoción Científica y Tecnológica (FONCYT) PICT 2017-0899, PICT 2015-3331 and the Secretaría de Ciencia y Técnica de la Universidad Nacional de Córdoba (SECyT-UNC). MFS and MCDP thank CONICET for their fellowships. MEO, MLG, SGR and JFM are Career Investigators of the Consejo Nacional de Investigaciones Científicas y Técnicas (CONICET).

The authors wish to acknowledge the assistance of the Consejo Nacional de Investigaciones Científicas y Técnicas (CONICET) and the Universidad Nacional de Córdoba, both of which provided support and facilities for this investigation.

The authors especially thank Paul Hobson, English native speaker, by revising the manuscript.

Author contributions

M.F.S. conceptualization, elaboration of systems and in-vivo and in-vitro experimental work, data analysis and writing the draft, review and editing; M.L.G. collaboration in in-vivo experimental work, and data analysis; J.F-M. and M.CDP. in-vitro experimental work and data analysis; C.L. collaboration in in-vivo experimental work and resources; E.A.S. data analysis, statistical analysis and writing; S.G-R. in-vitro experimental supervision, resources, and writing; M.E.O. conceptualization, supervision, project administration, resources, writing and review. All the authors contributed to the final revision and gave the final approval for the manuscript.

References

1. Wounds International. Best Practice Guidelines: Effective Skin and Wound Management of Non-complex Burns. *Wounds Int.* (2014).
2. Chantre, C. O. *et al.* Production-scale fibronectin nanofibers promote wound closure and tissue repair in a dermal mouse model. *Biomaterials* **166**, 96–108 (2018).
3. Norman, G. *et al.* Antiseptics for burns. *Cochrane database Syst. Rev.* **7**, CD011821 (2017).
4. Smith, R., Russo, J., Fiegel, J. & Brogden, N. Antibiotic Delivery Strategies to Treat Skin Infections When Innate Antimicrobial Defense Fails. *Antibiotics* **9**, 56 (2020).
5. Nímia, H. H. *et al.* Comparative study of Silver Sulfadiazine with other materials for healing and infection prevention in burns: A systematic review and meta-analysis. *Burns* **45**, 282–292 (2018).

6. Wasiak, J., Cleland, H., Campbell, F. & Spinks, A. Dressings for superficial and partial thickness burns. *Cochrane database Syst. Rev.* 1–85 (2013). doi:10.1002/14651858.CD002106.pub4.www.cochranelibrary.com
7. Saghazadeh, S. *et al.* Drug delivery systems and materials for wound healing applications. *Adv. Drug Deliv. Rev.* **127**, 138–166 (2018).
8. Ahmed, A., Getti, G. & Boateng, J. Ciprofloxacin-loaded calcium alginate wafers prepared by freeze-drying technique for potential healing of chronic diabetic foot ulcers. *Drug Deliv. Transl. Res.* **8**, 1751–1768 (2018).
9. Roy, D. C. *et al.* Ciprofloxacin-loaded keratin hydrogels reduce infection and support healing in a porcine partial-thickness thermal burn. *Wound Repair Regen.* **24**, 657–668 (2016).
10. Sanchez, M. F. *et al.* Ciprofloxacin-lidocaine-based hydrogel: development, characterization and in vivo evaluation in a second-degree burn model. *Drug Deliv. Transl. Res.* **8**, 1000–1013 (2018).
11. Sanchez, M. F., Guzman, M. L., Apas, A. L., Alovero, F. del L. & Olivera, M. E. Sustained dual release of ciprofloxacin and lidocaine from ionic exchange responding film based on alginate and hyaluronate for wound healing. *Eur. J. Pharm. Sci.* **161**, 105789 (2021).
12. Guo, X., Huang, S., Sun, J. & Wang, F. Comparison of the cytotoxicities and wound healing effects of hyaluronan, carbomer, and alginate on skin cells in vitro. *Adv. Skin Wound Care* **28**, 410–414 (2015).
13. Valachová, K. & Šoltés, L. Hyaluronan as a Prominent Biomolecule with Numerous Applications in Medicine. *International Journal of Molecular Sciences* **22**, (2021).
14. Garantziotis, S. & Savani, R. C. Hyaluronan biology: A complex balancing act of structure, function, location and context. *Matrix Biol.* **78–79**, 1–10 (2019).
15. Kevadiya, B. D. *et al.* Biodegradable gelatin-ciprofloxacin-montmorillonite composite hydrogels for controlled drug release and wound dressing application. *Colloids Surfaces B Biointerfaces* **122**, 175–183 (2014).
16. Lawrence, J. W. *et al.* Delayed Cytotoxicity and Cleavage Mammalian of Mitochondrial DNA in Ciprofloxacin-Treated Mamalian Cells. *Mol. Pharmacol.* **50**, 1178–1188 (1996).
17. Gürbay, A. *et al.* Cytotoxicity in ciprofloxacin-treated human fibroblast cells and protection by vitamin E. *Hum. Exp. Toxicol.* **21**, 635–641 (2002).
18. So, M. J., Hyun, Y. K. & Eun, J. C. Protective Role of Alginic Acid and Fucoidan from Nitric Oxide-Induced Oxidative Stress. *Agric. Sci.* **2**, 12–20 (2014).
19. Stellavato, A. *et al.* Positive Effects against UV-A Induced Damage and Oxidative Stress on an In Vitro Cell Model Using a Hyaluronic Acid Based Formulation Containing Amino Acids, Vitamins, and Minerals. *Biomed Res. Int.* 2018, 8481243 (2018).
20. Manzo, R. H., Jimenez Kairuz, A. F., Olivera, M. E., Alovero, F. L. & Ramirez-Rigo, M. V. Thermodynamic and Rheological Properties of Polyelectrolyte Systems. in *Polyelectrolytes, Thermodynamics and Rheology* (eds. Visakh, P., Bayraktar, O. & Picó, G. A.) 215–244 (Springer International Publishing, 2014). doi:10.1007/978-3-319-01680-1_6

21. Chen, T., Tsai, T. & Chang, S. Molecular mechanism of fluoroquinolones modulation on corneal fibroblast motility. *Exp. Eye Res.* **145**, 10–16 (2016).
22. Khorshid, F. A. The effect of the medium viscosity on the cells morphology in reaction of cells to topography - I. *Proc. 2nd Saudi Sci. Conf.* **98**, 67–98 (2005).
23. Zhao, X.-K. *et al.* Focal Adhesion Kinase Regulates Fibroblast Migration via Integrin beta-1 and Plays a Central Role in Fibrosis. *Sci. Rep.* **6**, 19276 (2016).
24. Boo, S. & Dagnino, L. Integrins as Modulators of Transforming Growth Factor Beta Signaling in Dermal Fibroblasts During Skin Regeneration After Injury. *Advances in wound care* **2**, 238–246 (2013).
25. Yergoz, F. *et al.* Heparin mimetic peptide nanofiber gel promotes regeneration of full thickness burn injury. *Biomaterials* **134**, 117–127 (2017).
26. Kushibiki, T. *et al.* Photocrosslinked gelatin hydrogel improves wound healing and skin flap survival by the sustained release of basic fibroblast growth factor. *Sci. Rep.* **11**, 23094 (2021).
27. Devalliere, J. *et al.* Co-delivery of a growth factor and a tissue-protective molecule using elastin biopolymers accelerates wound healing in diabetic mice. *Biomaterials* **141**, 149–160 (2017).
28. Wang, Y. *et al.* Burn injury: Challenges and advances in burn wound healing, infection, pain and scarring. *Adv. Drug Deliv. Rev.* **123**, 3–17 (2018).
29. Boateng, J. & Catanzano, O. Advanced Therapeutic Dressings for Effective Wound Healing - A Review. *J. Pharm. Sci.* **104**, 3653–3680 (2015).
30. Hoeksema, H., Vandekerckhove, D., Verbelen, J., Heyneman, A. & Monstrey, S. A comparative study of 1% silver sulphadiazine (Flammazine) versus an enzyme alginogel (Flaminal) in the treatment of partial thickness burns. *Burns* **39**, 1234–1241 (2013).
31. Koehler, J., Brandl, F. P. & Goepferich, A. M. Hydrogel wound dressings for bioactive treatment of acute and chronic wounds. *Eur. Polym. J.* **100**, 1–11 (2018).
32. Stoica, A. E., Chircov, C. & Grumezescu, A. M. Hydrogel Dressings for the Treatment of Burn Wounds: An Up-To-Date Overview. *Materials (Basel).* **13**, 2853 (2020).
33. Day, R. M. Functional requirements of wound repair biomaterials. in *Woodhead Publishing Series in Biomaterials* (ed. Farrar, D. B. T.-A. W. R. T.) 155–173 (Woodhead Publishing, 2011). doi:https://doi.org/10.1533/9780857093301.2.155
34. Madaghiele, M., Demitri, C., Sannino, A. & Ambrosio, L. Polymeric hydrogels for burn wound care: Advanced skin wound dressings and regenerative templates. *Burn. Trauma* **2**, 153–161 (2014).
35. Coats, T. J., Edwards, C., Newton, R. & Staun, E. The effect of gel burns dressings on skin temperature. *Emerg. Med. J.* **19**, 224–225 (2002).
36. Chang, S.-J., Sartika, D., Fan, G.-Y., Cherng, J.-H. & Wang, Y. Animal Models of Burn Wound Management. in *Animal Models in Medicine and Biology* (IntechOpen, 2019). doi:10.5772/intechopen.89188

37. Volkova, N., Yukhta, M., Pavlovich, O. & Goltsev, A. Application of Cryopreserved Fibroblast Culture with Au Nanoparticles to Treat Burns. *Nanoscale Res. Lett.* **11**, 22 (2016).
38. Jin, G., Prabhakaran, M. P., Kai, D. & Ramakrishna, S. Controlled release of multiple epidermal induction factors through core – shell nanofibers for skin regeneration. *Eur. J. Pharm. Biopharm.* **85**, 689–698 (2013).
39. Ministerio de Salud; Secretaría de Políticas Regulación e Institutos; Administración Nacional de Medicamentos Alimentos y Tecnología Médica; Instituto Nacional de Medicamentos. Farmacopea Argentina. in *Farmacopea Agentina* 0–175 (2010).
40. Olivera, M. E. *et al.* Biowaiver monographs for immediate release solid oral dosage forms: ciprofloxacin hydrochloride. *J. Pharm. Sci.* **100**, 22–33 (2011).
41. Bravo-Miana, R. D. C. *et al.* Thyroid tumor cells-fibroblasts crosstalk: role of extracellular vesicles. *Endocr. Connect.* **9**, 506–518 (2020).
42. ISO 10993-5: Biological evaluation of medical devices. Part 5: Tests for in vitro cytotoxicity. *International Organization for Standardization*. (2009).
43. Flores-Martín, J., Rena, V., Márquez, S., Panzetta-Dutari, G. M. & Genti-Raimondi, S. StarD7 Knockdown Modulates ABCG2 Expression, Cell Migration, Proliferation, and Differentiation of Human Choriocarcinoma JEG-3 Cells. *PLoS One* **7**, e44152 (2012).
44. Yaman, I., Durmus, a S., Ceribasi, S. & Yaman, M. Effects of Nigella sativa and silver sulfadiazine on burn wound healing in rats. *Vet. Med. (Praha).* **55**, 619–624 (2010).
45. National Research Council (US) Committee for the Update of the Guide for the Care and Use of Laboratory Animals. Guide for the Care and Use of Laboratory Animals. 1–246 (2011). doi:10.17226/12910

Figures

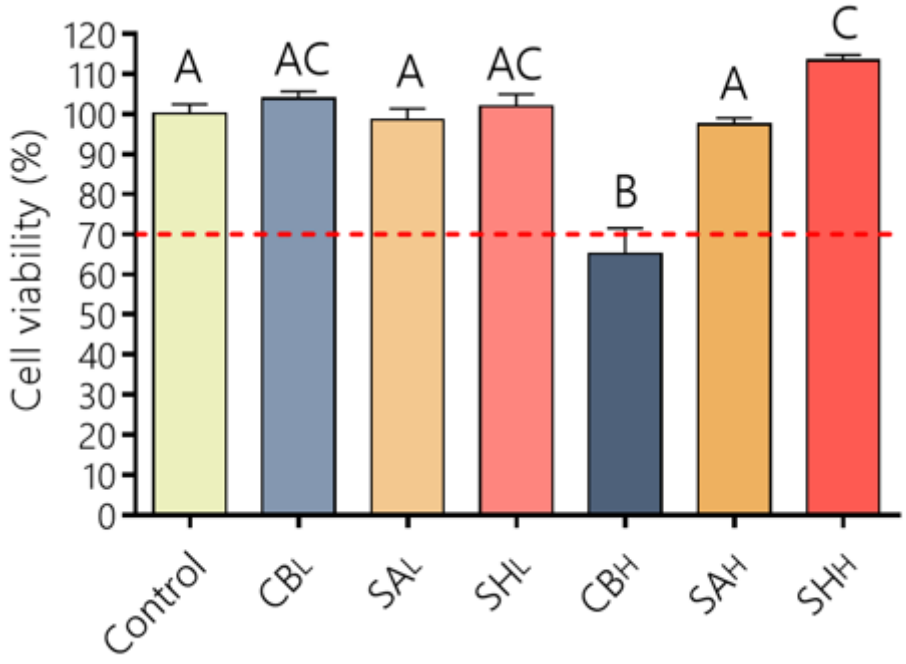

Figure 1

Effect of PE_L and PE_H on CV% of HDF cells after 24 hours of treatment. The CV% was calculated from Equation 1. Values are expressed as the means ± their standard errors (n=8). Differences between the treatments were evaluated with ANOVA and Tukey's post-test ($p<0.05$), with different capital letters above the bars indicating significant differences. The dotted line determines the cell viability limit allowed by ISO 10993 5 (CV≥ 70%).

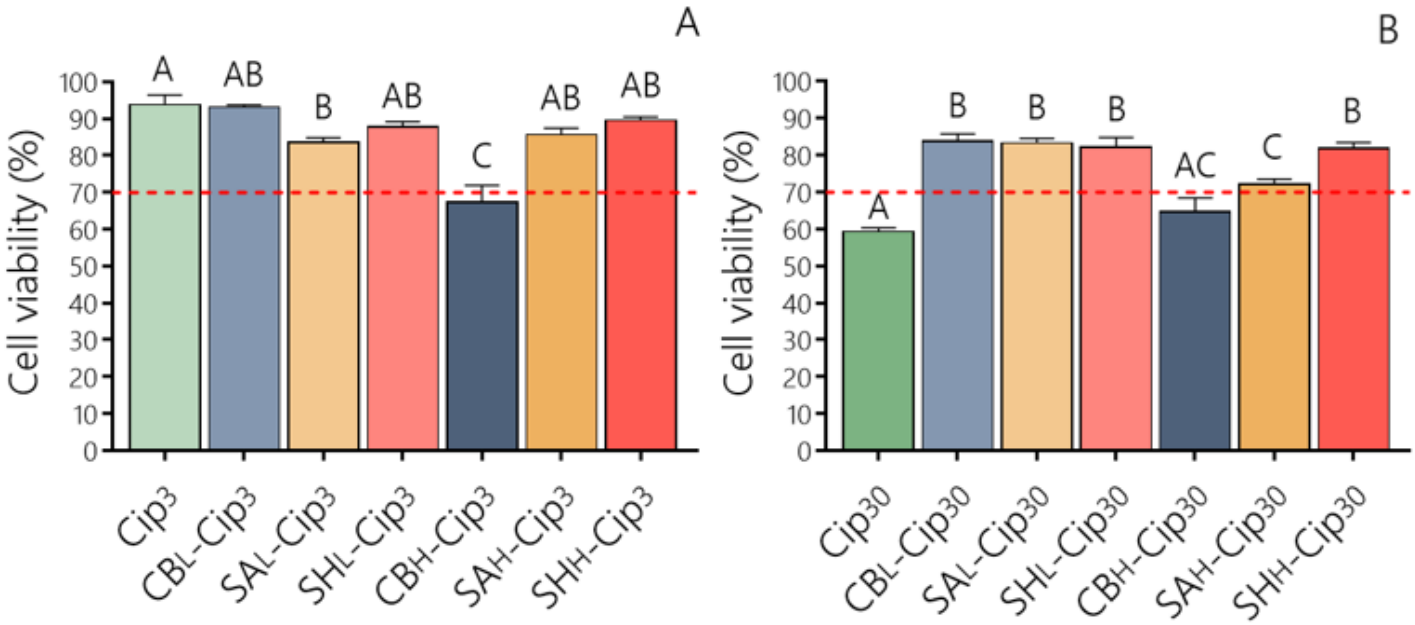

Figure 2

Cell viability of HDFs after 24 hours of treatment with A) Cip_3 and its complexes with PE_L or PE_H, and B) Cip_{30} and its complexes with PE_L or PE_H. The CV% was calculated according to Equation 1. Values are expressed as the means ± their standard errors (n=8). Differences between the treatments were evaluated by ANOVA and Tukey's post-test ($p<0.05$), with different capital letters above the bars indicating significant differences. The dotted line determines the cell viability limit allowed by ISO 10993 5 (CV≥ 70%).

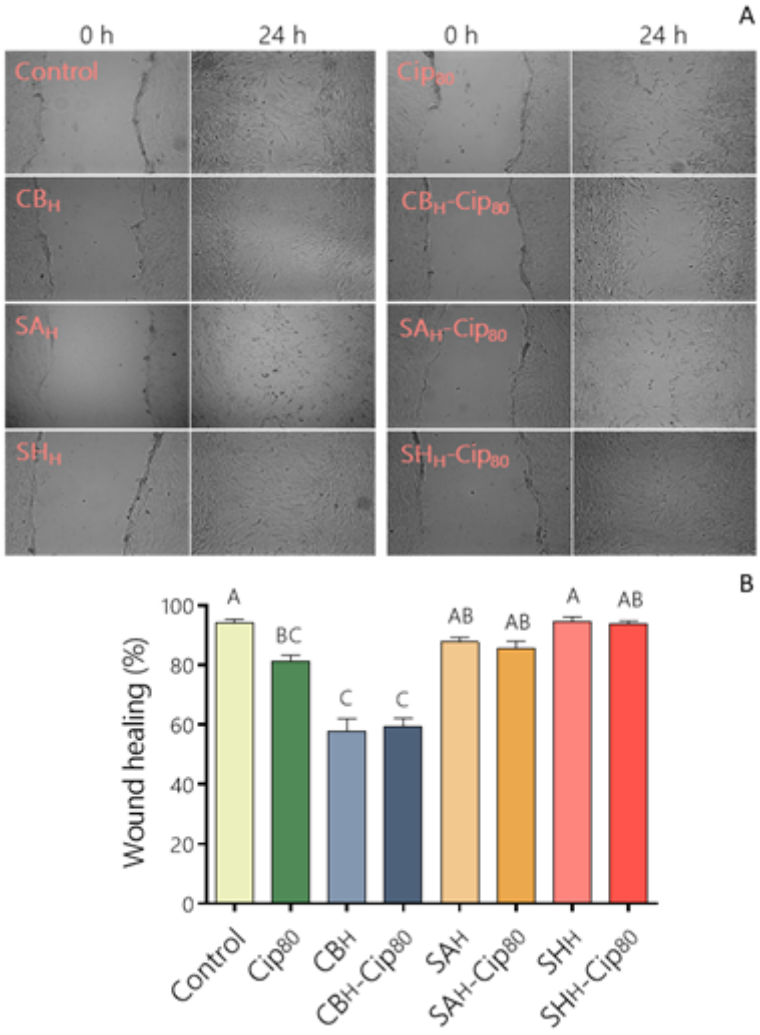

Figure 3

Effect of CB, SA, SH, or PE-Cip complexes on cell migration. A) Representative images of wound healing assays performed on HDF cells treated as indicated. An open furrow was generated by scratching confluent cells using a pipette tip, and cells images were obtained at the initial time and after 24 h. B) The distance between furrow edges in control or treated cells of three independent experiments was measured and presented graphically as the percentage of the initial distance (0 h); *$p<0.05$ compared to control cells.

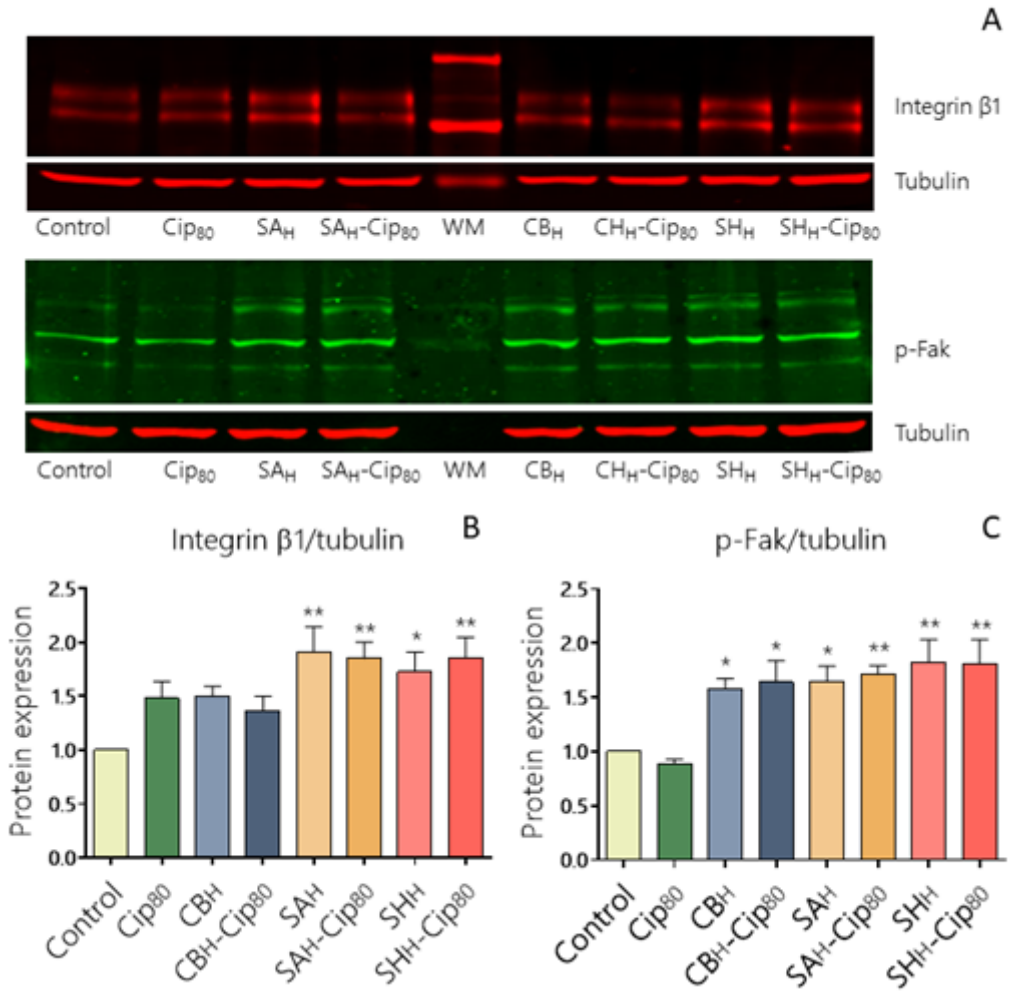

Figure 4

Effect of Cip, PE or PE-Cip complexes on integrin β1 and p-FAK protein expression. (A) Protein expression was analyzed by Western blot assays from cell lysates (100 µg/lane) of HDF-treated cells electrophoresed on a 7.5% SDS-PAGE and transferred to a nitrocellulose filter. Filters were incubated with anti-integrin β1, anti-p-FAK or anti-α-tubulin antibodies. Representative blot of three independent experiments with similar results is shown. Cropped blots from different parts of the same gel are separated by white spaces. (B-C) The bar graphs represent the densitometric quantification of protein levels in treated cells normalized to α-tubulin of three separate experiments compared to the corresponding normalized protein levels in control cells defined as 1 (mean ± SEM). Differences in treatments were evaluated using ANOVA with Dunnett's post-test *p<0.05; **p<0.01.

Figure 5

See image above for figure legend.

Figure 6

See image above for figure legend.

Figure 7

See image above for figure legend.

Figure 8

Representative photomicrographs of burn wounds for the NT group and after treatment with R-cream, AA-films, C-films or AA-hydrogel. H&E (×100, scale bars are 100 μm).

Figure 9

Biopsy location. The wounds were divided into 4 parts with two imaginary lines. Biopsies were taken clockwise from the center of each part (according to day 0) on days 0, 7, 14, and 21. Thus, each animal was its own control, and in this way we managed to reduce the number of experimental animals used, according to the Guide for the Care and Use of Experimental Animals.